

RESEARCH ARTICLE

Backward flight in hummingbirds employs unique kinematic adjustments and entails low metabolic cost

Nir Sapir^{1,*} and Robert Dudley^{1,2}

¹Department of Integrative Biology, University of California, Berkeley, CA 94720, USA and ²Smithsonian Tropical Research Institute, Balboa, Republic of Panama

*Author for correspondence (nir.sapir@berkeley.edu)

SUMMARY

Backward flight is a frequently used transient flight behavior among members of the species-rich hummingbird family (Trochilidae) when retreating from flowers, and is known from a variety of other avian and hexapod taxa, but the biomechanics of this intriguing locomotor mode have not been described. We measured rates of oxygen uptake (\dot{V}_{O_2}) and flight kinematics of Anna's hummingbirds, *Calypte anna* (Lesson), within a wind tunnel using mask respirometry and high-speed videography, respectively, during backward, forward and hovering flight. We unexpectedly found that \dot{V}_{O_2} in sustained backward flight is similar to that in forward flight at equivalent airspeed, and is about 20% lower than hovering \dot{V}_{O_2} . For a bird that was measured throughout a range of backward airspeeds up to a speed of 4.5 ms^{-1} , the power curve resembled that of forward flight at equivalent airspeeds. Backward flight was facilitated by steep body angles coupled with substantial head flexion, and was also characterized by a higher wingbeat frequency, a flat stroke plane angle relative to horizontal, a high stroke plane angle relative to the longitudinal body axis, a high ratio of maximum:minimum wing positional angle, and a high upstroke:downstroke duration ratio. Because of the convergent evolution of hummingbird and some hexapod flight styles, flying insects may employ similar kinematics while engaged in backward flight, for example during station keeping or load lifting. We propose that backward flight behavior in retreat from flowers, together with other anatomical, physiological, morphological and behavioral adaptations, enables hummingbirds to maintain strictly aerial nectarivory.

Supplementary material available online at <http://jeb.biologists.org/cgi/content/full/215/20/3603/DC1>

Key words: avian locomotor mode, *Calypte anna*, flight agility, mask respirometry, mass-specific metabolic rate, nectarivory.

Received 27 March 2012; Accepted 3 July 2012

INTRODUCTION

Although backward walking and running have been characterized in various terrestrial taxa (Ashley-Ross and Lauder, 1997; Buford and Smith, 1990; Cavagna et al., 2011; Grasso et al., 1998; Vilensky and Cook, 2000), the biomechanics of backward flight have not yet been described. Backward flight is prevalent as a transient flight behavior in the species-rich hummingbird family Trochilidae and in other avian families that routinely retreat from flowers after nectar feeding, as well as in various hexapod taxa (Davey and Davey, 1945; Frina et al., 1995; Greenewalt, 1960a; Nachtigall, 1998; Ng'weno, 1990; Yokoi and Fujisaki, 2009; Zeil and Wittmann, 1989). Hummingbird feeding typically involves forward flight while approaching a flower, hovering almost motionless during feeding, and backward flight when retreating; hence, backward flight is carried out by hummingbirds many dozens of times each day. In addition, hummingbirds occasionally fly backwards during aerial agonistic interactions with other hummingbirds. In volant hexapods, backward flight has been described during station keeping, load lifting and evasion from predators (Nachtigall, 1998; Yokoi and Fujisaki, 2009; Zeil and Wittmann, 1989). The metabolic rate of birds in general, and of hummingbirds in particular, is known for slow forward flight to be lower than that during hovering (Askew and Ellerby, 2007; Clark and Dudley, 2010; Dial et al., 1997; Pennycuik, 1968; Tobalske et al., 2003), with correspondingly altered wing and body kinematics (e.g. lower body angle and higher

stroke plane angle relative to horizontal) (e.g. Tobalske et al., 2007), but the comparable costs of backward flight are unknown.

Studies of humans and some tetrapods have revealed diverse kinematic strategies employed during backward locomotion (Ashley-Ross and Lauder, 1997; Buford and Smith, 1990; Cavagna et al., 2011; Grasso et al., 1998; Vilensky and Cook, 2000). Additionally, backward walking and running are energetically 28–78% and 15–34%, respectively, more demanding than their forward locomotion equivalents, as a result of greater external work done against gravity at low speeds and greater internal work caused by an increased step frequency and greater mass-specific vertical stiffness of the bouncing system at high speeds (Cavagna et al., 2012; Flynn et al., 1994; Vilensky et al., 1987; Williford et al., 1998; Winter et al., 1989). The elevated metabolic demands associated with backward movement likely derive from the relative terrestrial rarity of this locomotor mode. By contrast, such demands may be negligible for hummingbirds for which this aerial behavior occurs frequently. To this end, we measured oxygen uptake rate (\dot{V}_{O_2}) and flight kinematics of Anna's hummingbirds (*Calypte anna*) within a wind tunnel using respirometry and high-speed videography, respectively, during backward and forward flight (both at an airspeed of 3 ms^{-1}), and for still-air hovering (Fig. 1A). In addition, we repeated this for one bird throughout a range of backward flight speeds.

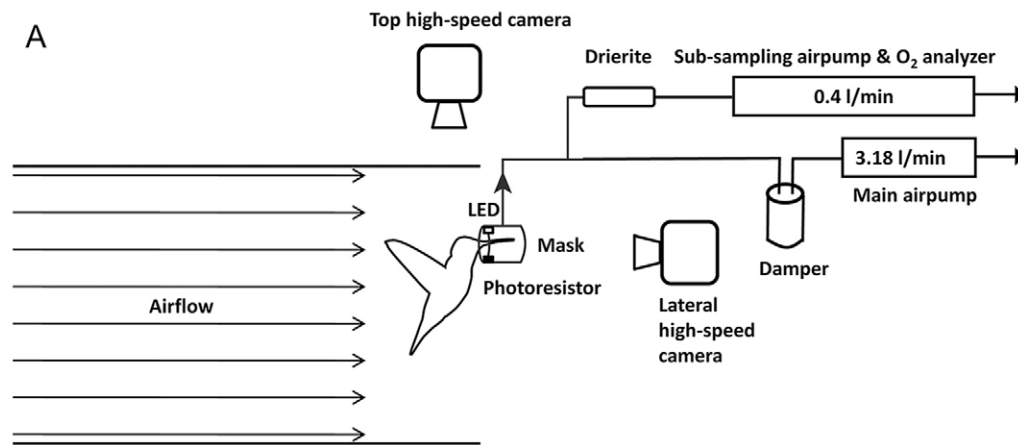


Fig. 1. (A) General setup of the wind tunnel in which Anna's hummingbirds were studied using respirometry and high-speed videography during backward, forward and still-air flights. (B) Photograph of an Anna's hummingbird during feeding from the respirometry mask.



MATERIALS AND METHODS

This research was conducted in compliance with the University of California, Berkeley's Animal Use Protocol R282-0310. Bird trapping and housing were under permits from the United States Fish and Wildlife Service (permit no. MB054440-0) and California Department of Fish and Game (permit no. SC-006627). During January to April 2011, five male Anna's hummingbirds (mean \pm s.d. body mass 4.59 ± 0.22 g) were trapped at the UC campus in Berkeley, CA, USA, and were held for 1–7 weeks before being released back into the wild. Values of \dot{V}_{O_2} for all treatments on any given individual bird were measured over a combined duration of several hours in one day using an open-circuit wind tunnel (Model 404, Engineering Laboratory Design, Lake City, MN, USA) with a $45.5 \times 45.5 \times 91.5$ cm working section. On a subsequent day, we used high-speed flight videography (Fig. 1A) to extract kinematic variables (Fig. 2) within the same experimental volume. The feeder was placed *ca.* 15 cm from the test section ceiling either facing or opposite the flow, permitting backward and forward flight, respectively. Birds flew in the wind tunnel under four experimental treatments: (1) backward flight at an airspeed of 3 m s^{-1} , (2) still-air hovering flight using the same feeder position, (3) forward flight at an airspeed of 3 m s^{-1} , and (4) still-air hovering flight using the same feeder position. Therefore, our experimental protocol included two still-air hovering treatments in which the feeder direction differed by 180° in relation to the longitudinal axis of the wind tunnel. We selected to compare backward and forward flight at an airspeed of 3 m s^{-1} because various flight characteristics, including metabolic rate, wingbeat frequency and advance ratio are known to be similar during slow forward ($\leq 1.5 \text{ m s}^{-1}$) and hovering flight (Ellington, 1984; Tobalske et al., 2007; Clark and Dudley, 2010). By contrast, increasing the airspeed to 3 m s^{-1} elicits non-hovering flight situations that are also similar to airspeeds recorded from

hummingbirds retreating backward from flowers with backward airspeeds of up to 2.0 m s^{-1} (N.S., unpublished data). In addition, one of the birds was flown over a range of backward airspeeds from 0 to 4.5 m s^{-1} during which it was videographed and its \dot{V}_{O_2} was measured. Indeed, metabolic and kinematic variables were very similar for this individual tested in still-air hovering and at a backward flight speed of 1.5 m s^{-1} (see Results). This individual could not fly backward at 6 m s^{-1} and also feed from the feeder. The airspeed of 3 m s^{-1} thus represents a reasonable compromise between hovering flight and airspeed limits to backward flight.

Values of \dot{V}_{O_2} were determined using a respirometry mask (Bartholomew and Lighton, 1986; Berger and Hart, 1972; Clark and Dudley, 2010; Lighton, 2008; Welch, 2011). The mask was made from a 20 ml syringe cut to one-third of its length and positioned horizontally such that the bird could position its head within the syringe's lumen. The tip of the 20 ml syringe, located at the rear of the mask, was connected to the tip of a 10 ml syringe that was filled with hummingbird nectar (Nektar-Plus, Nekton, Pforzheim, Germany), allowing free access to nectar. From the inner bottom part of the mask, a tube was connected to a dedicated airpump (UN73, Neuberger KNF, Freiburg, Germany) such that expired air was pulled through the mask during nectar feeding (Fig. 1). Air was sub-sampled from the airflow tube using a FoxBox (Sable Systems International, Las Vegas, NV, USA) that determined % O_2 of the airstream following scrubbing of water vapor using Drierite (W. A. Hammond Drierite, Xenia, OH, USA). Airflow through the mask was measured using a flowmeter (model 32446-33, Cole-Parmer, Vernon Hills, IL, USA) calibrated with a mass-flow calibrator (1E4-VCR-V-Q, DH Instruments Inc., Phoenix, AZ, USA). Mask airflow averaged 3.58 l min^{-1} .

Oxygen depletion relative to the ambient atmospheric level was integrated over time using ExpeData software (Sable Systems

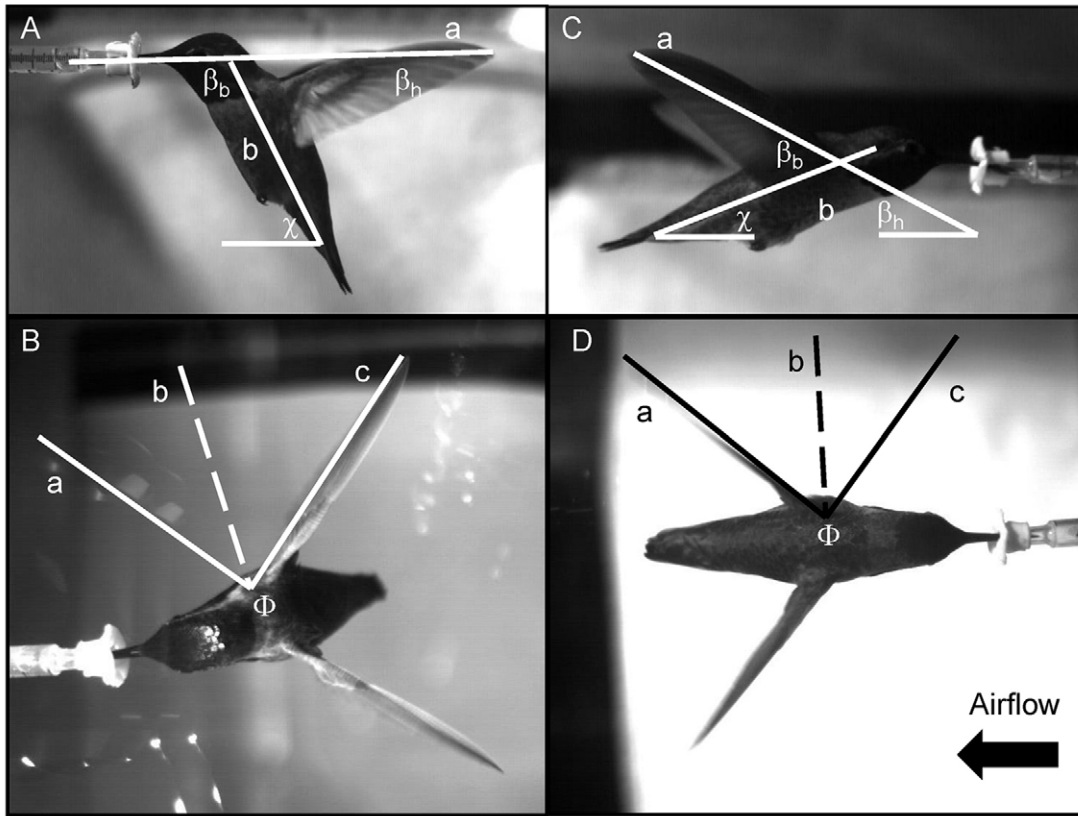


Fig. 2. Video frames of an Anna's hummingbird during backward and forward flight at an airspeed of 3 m s^{-1} , taken from lateral and vertically downward directed (top) high-speed cameras. For a photograph of the respirometry mask used see Fig. 1B. (A) Image of the lateral camera during hummingbird feeding at backward flight, with line 'a' connecting the wing tip at the end of the upstroke (as can be seen in the photograph) and at the end of the downstroke (the other end of the line). The angle of this line relative to horizontal is the wing stroke plane in relation to horizontal (β_h). The wing stroke plane in relation to the longitudinal body axis (β_b) is given by the angle of this line in relation to 'b', the longitudinal body axis, which, in relation to horizontal, is defined as the body angle (χ). (B) Image of the top camera during hummingbird feeding at backward flight, with 'a' depicting the end of downstroke positional angle (Φ_{\min}), 'b' depicting a line perpendicular to the body that is used to measure the fore and rear parts of the wingbeat cycle, and 'c' depicting the end of upstroke wing positional angle (Φ_{\max}). The wingbeat amplitude (Φ) is the angle between 'a' and 'c'. Φ , Φ_{\min} and Φ_{\max} were calculated in relation to the horizontal stroke plane angle (β_h) and not relative to horizontal. (C) Image of the lateral camera during hummingbird feeding at forward flight. For the definition of the different angles, see A. (D) Image of the top camera during hummingbird feeding at forward flight. For the definition of the different angles, see B. Airflow direction for all photos is indicated by a black arrow in the lower right corner of D.

International) to yield the total volume of consumed O_2 . The instantaneous value of \dot{V}_{O_2} was calculated following Withers (Withers, 1977):

$$\dot{V}_{\text{O}_2} = \dot{V}_{\text{E}} \left(\frac{F_{\text{I}\text{O}_2} - F_{\text{E}\text{O}_2}}{1 - F_{\text{I}\text{O}_2}} \right), \quad (1)$$

where \dot{V}_{E} is the mass flow of gas exiting the mask, $F_{\text{I}\text{O}_2}$ represents the fractional concentration of O_2 entering the mask and $F_{\text{E}\text{O}_2}$ represents the fractional concentration of O_2 exiting the mask. We used a photoresistor/LED pair attached to the feeder's opening (Bartholomew and Lighton, 1986; Welch, 2011) (see Fig. 1A), which was monitored electronically *via* the FoxBox to determine the duration of head insertion within the mask. The respiratory exchange ratio (RER) was assumed to be unity (see Welch et al., 2007).

Total O_2 consumed during a feeding bout was divided by the total duration of the feeding time within the mask to calculate the overall net rate of oxygen uptake. Following previous methods (Bartholomew and Lighton, 1986), we excluded those measurements for which the feeding duration within the mask was too short for reliable \dot{V}_{O_2} determination (i.e. $< 2 \text{ s}$). We present the mean \pm s.d. \dot{V}_{O_2} in the form of mass-specific metabolic rate (in $\text{ml O}_2 \text{ h}^{-1} \text{ g}^{-1}$ of

bird body mass). Bird body mass was measured before and after daily experimental sessions and body mass used in our calculations is the mean of the two measurements. To transform \dot{V}_{O_2} to power in watts, we used a conversion factor of $20.9 \text{ kJ l}^{-1} \text{ O}_2$ catabolized energy (see Walsberg and Wolf, 1995).

Clark and Dudley (Clark and Dudley, 2010) determined that mask airflow rates $> 3 \text{ l min}^{-1}$ were sufficient to capture respiratory gases from hummingbirds even during a high forward airspeed of 10 m s^{-1} , whereas lower airspeeds, as characterize the present study, required much lower flow rates. To further validate respirometry measurements, we measured the dilution of airflow under different experimental conditions using a standardized procedure. We used a gas cylinder of pure argon connected to a flow regulator that maintained a constant flow rate of 0.02 l min^{-1} , as continuously measured by the above-mentioned flowmeter. Argon flowed through a tube such that its tip was transiently inserted into the mask for a mean \pm s.d. duration of $7.6 \pm 2.5 \text{ s}$. Because of the dilution of atmospheric air by the argon influx, we were able to measure 'virtual \dot{V}_{O_2} ' (see Lighton, 2008), using FoxBox and ExpeData readings of % O_2 , Eqn 1, and the duration of tube insertion recorded by the photoresistor/LED pair, as described above. We tested whether

Table 1. Mean \pm s.d. data and results of two-way mixed ANOVA in which mass-specific oxygen uptake rate and kinematic variables of Anna's hummingbirds were compared during backward flight (-3 m s^{-1}) and forward flight ($+3\text{ m s}^{-1}$) and during two different still-air hovering flight treatments in which the feeder was in either backward or forward position

Variable	-3 m s^{-1}	0 m s^{-1} (backward position)	0 m s^{-1} (forward position)	$+3\text{ m s}^{-1}$	<i>F</i> treatment	<i>F</i> individual	<i>F</i> treatment \times individual
Mass-specific metabolic rate ($\text{ml O}_2\text{ g}^{-1}\text{ h}^{-1}$)	48.6 \pm 6.9 ^A	58.1 \pm 8.5 ^B	59.7 \pm 10.1 ^B	46.6 \pm 8.3 ^A	26.7***	40.3***	4.6***
χ	70.6 \pm 9.7 ^A	53.2 \pm 5.2 ^B	52.2 \pm 4.5 ^B	37.6 \pm 3.8 ^C	44.5***	3.1 ^{n.s.}	3.6**
λ_b	64.8 \pm 4.0 ^A	51.4 \pm 4.3 ^B	51.0 \pm 5.0 ^B	41.6 \pm 4.9 ^C	46.0***	3.3*	2.9**
β_h	-0.1 ± 6.9^A	9.3 \pm 5.3 ^B	11.9 \pm 3.3 ^C	21.1 \pm 5.8 ^D	48.7***	12.9***	5.1***
β_b	70.5 \pm 11.2 ^A	62.5 \pm 6.7 ^{B,C}	64.1 \pm 3.5 ^B	58.7 \pm 7.1 ^C	4.3*	4.3*	4.2***
Φ	130.3 \pm 7.6 ^A	134.7 \pm 7.3 ^{A,B}	135.8 \pm 8.2 ^B	123.0 \pm 9.6 ^C	7.8**	7.1**	2.3*
$\Phi_{\text{max}}:\Phi_{\text{min}}$	1.31 \pm 0.24 ^A	1.16 \pm 0.18 ^B	1.18 \pm 0.12 ^B	1.16 \pm 0.18 ^B	2.7 ^{n.s.}	9.9**	2.1*
<i>f</i> (Hz)	43.8 \pm 2.5 ^A	42.1 \pm 1.2 ^B	42.2 \pm 1.3 ^B	39.7 \pm 1.7 ^C	15.6***	5.3**	1.4 ^{n.s.}
<i>J</i>	0.29 \pm 0.01 ^A	–	–	0.34 \pm 0.02 ^B	30.1**	1.8 ^{n.s.}	10.8***
US:DS	1.13 \pm 0.10 ^A	0.98 \pm 0.06 ^B	1.00 \pm 0.09 ^B	1.01 \pm 0.10 ^B	–	–	–

χ , body angle; λ_b , ventral head flexion; β_h , stroke plane angle in relation to horizontal; β_b , stroke plane angle in relation to longitudinal body axis; Φ , wingbeat amplitude; $\Phi_{\text{max}}:\Phi_{\text{min}}$, ratio maximum:minimum wing positional angle; *f*, wingbeat frequency; *J*, advance ratio; US:DS, ratio of upstroke:downstroke duration. Advance ratio *J* is defined as $V/(2\Phi fR)$, where *V* is airspeed in m s^{-1} , Φ is the wingbeat amplitude in radians, *f* is the wingbeat frequency and *R* is wing length. n.s., not significant; * $0.05 < P < 0.01$, ** $0.01 < P < 0.001$, *** $P < 0.001$.

Different superscript letters indicate different statistical groups based on Bonferroni *post hoc* comparisons ($P < 0.05$). All ANOVA models included an intercept term (not listed in the table).

Degrees of freedom (d.f.) in the mass-specific metabolic rate model are: treatment (3,12), individual (4,12) and treatment \times individual (12,80). d.f. in all kinematic variable models except for advance ratio are: treatment (3,12), individual (4,12) and treatment \times individual (12,40). d.f. in the advance ratio model are: treatment (1,4), individual (4,4) and treatment \times individual (4,20).

Upstroke:downstroke duration was tested using a Kruskal–Wallis non-parametric test with the independent factor treatment because the data were not normally distributed (Kolmogorov–Smirnov test, $P < 0.001$). Model results: $\chi^2 = 20.84$, $P < 0.001$. Different superscript letters indicate different statistical groups based on Kruskal–Wallis *post hoc* comparisons (Siegel and Castellan, 1988) with critical $P < 0.05$.

'virtual \dot{V}_{O_2} ' differed among backward flight at 3 m s^{-1} , forward flight at 3 m s^{-1} and still-air hovering. No significance difference in 'virtual \dot{V}_{O_2} ' was found between the three flight conditions (one-way ANOVA, $N=6$ replicate measurements from each of the three treatments, $F_{2,17}=0.35$, $P=0.7$).

Still video frames from two (top and lateral) synchronized high-speed (500 frames s^{-1}) cameras (X-PRI, AOS Technologies AG, Baden Daettwil, Switzerland) and ImageJ software (version 1.43u, National Institutes of Health, USA) were used to determine kinematic variables (Dudley, 1992; Ellington, 1984) from flying birds that fed from a horizontal 1 ml syringe filled with hummingbird nectar. The kinematic variables consisted of body angle in relation to horizontal (χ), head flexion in relation to the longitudinal body axis (λ_b), stroke plane angle in relation to horizontal (β_h), stroke plane angle in relation to the longitudinal body axis (β_b), wingbeat amplitude (Φ), ratio of maximum to minimum wing positional angle ($\Phi_{\text{max}}:\Phi_{\text{min}}$), wingbeat frequency (*f*), upstroke-to-downstroke duration ratio (US:DS) and advance ratio (*J*). The advance ratio is the ratio of the forward flight velocity to the mean flapping velocity of the wing tip, calculated following Ellington (Ellington, 1984):

$$J = \frac{V}{2\Phi fR}, \quad (2)$$

where *V* is airspeed in m s^{-1} , Φ is the wingbeat amplitude in radians, *f* is the wingbeat frequency and *R* is wing length. Ellington suggested that slow forward flight aerodynamically similar to hovering is characterized by values of *J* less than 0.1, while *J* near or exceeding unity characterizes fast forward flight (Ellington, 1984).

Values of \dot{V}_{O_2} and all kinematic variables were measured five and three times, respectively, for each treatment on each individual bird. For the one bird that was measured over the full range of backward airspeeds, values of \dot{V}_{O_2} and all kinematic variables were measured six and four times, respectively, for each airspeed. We note that hummingbirds filmed during feeding from either syringe

feeders or respirometry masks constantly moved their bills in small displacements, and did not obviously seem to hang from feeders with their bills at any airspeed. For statistical analyses, we applied two-way mixed ANOVA with treatment as an independent fixed factor, and individual as an independent random factor, followed by Bonferroni *post hoc* comparisons, using SPSS (version 15.0, SPSS Inc., Chicago, IL, USA). As the US:DS data distribution significantly deviated from normal (Kolmogorov–Smirnov test, $Z=2.779$, $P < 0.001$), we applied a non-parametric Kruskal–Wallis test using SPSS, followed by *post hoc* comparisons (Siegel and Castellan, 1988). We did not statistically test results from the one bird that was measured over the full range of backward airspeeds given this restricted sample size. All tests were two-tailed with critical $\alpha=0.05$.

Because body angle in relation to the airflow angle influences parasite drag of the flying bird, the steep body angles (~ 70 deg) employed during backward flight may result in high body drag. To test for this effect, we measured drag forces on a life-sized model of an Anna's hummingbird positioned at 37.6 deg into a 3 m s^{-1} airflow, and at a 70.6 deg pointing away from 3 m s^{-1} airflow, which correspond to average forward and backward flight positions of hummingbirds in our experiments, respectively (see Fig. 2A,C, Table 1; supplementary material Movies 1, 2). We used photographs of one *C. anna* to design a 3D model (Blender, The Blender Foundation, www.blender.org), which was then printed using a rapid prototyping machine (Projet HD 3000, 3D Systems, Rock Hill, SC, USA). The model (with a tail but no wings) was mounted on a six degrees-of-freedom force and torque sensor (Nano17, ATI, Apex, NC, USA) to measure body drag. Parasite power was then given by the product of drag and airspeed.

RESULTS

Hummingbirds performed voluntary and sustained backward flights that lasted (mean \pm s.d.) $18.0\pm 6.2\text{ s}$ ($N=25$ flights from five

Table 2. Mean \pm s.d. mass-specific oxygen uptake rate and kinematic variables of an Anna's hummingbird during variable backward flight airspeeds

Variable	0 m s ⁻¹	1.5 m s ⁻¹	3 m s ⁻¹	4.5 m s ⁻¹
Mass-specific metabolic rate (ml O ₂ g ⁻¹ h ⁻¹)	44.3 \pm 2.1	42.1 \pm 2.8	38.9 \pm 1.9	38.3 \pm 1.5
χ	49.7 \pm 5.4	50.8 \pm 4.8	62.3 \pm 2.1	75.2 \pm 3.9
λ_b	58.1 \pm 5.0	52.2 \pm 5.4	58.7 \pm 2.1	72.9 \pm 6.9
β_h	6.2 \pm 1.7	6.0 \pm 1.1	-2.2 \pm 1.9	-15.3 \pm 4.0
β_b	55.9 \pm 6.0	56.8 \pm 4.8	60.1 \pm 2.0	60.0 \pm 3.0
Φ	125.9 \pm 7.5	122.6 \pm 3.1	128.5 \pm 2.4	129.0 \pm 2.6
$\Phi_{\max}:\Phi_{\min}$	1.5 \pm 0.16	1.44 \pm 0.28	1.64 \pm 0.004	1.4 \pm 0.34
f (Hz)	43.2 \pm 1.6	43.9 \pm 0.6	43.7 \pm 0.4	46.2 \pm 0.6
J	—	0.31 \pm 0.01	0.30 \pm 0.01	0.28 \pm 0.01
US:DS	0.92 \pm 0.10	0.92 \pm 0.10	1.05 \pm 0.10	0.83 \pm 0.002

Advance ratio J is defined as $V/(2\Phi fR)$, where V is airspeed in m s⁻¹, Φ is the wingbeat amplitude in radians, f is the wingbeat frequency and R is wing length. For other definitions, see Table 1.

individuals), during which the duration of head insertion into the respirometry mask averaged 10.8 \pm 4.0 s. The birds necessitated no training to fly backwards. At an airspeed of 3 m s⁻¹, \dot{V}_{O_2} did not differ significantly between backward (supplementary material Movie 1) and forward (supplementary material Movie 2) flight, and both rates were about 20% lower than during hovering (Fig. 3A, Table 1; supplementary material Movie 3). Power input (mean \pm s.d.) during backward, hovering and forward flight was 1.280 \pm 0.179, 1.542 \pm 0.208 and 1.211 \pm 0.173 W, respectively. Values of \dot{V}_{O_2} found in this study during forward and hovering flight (Fig. 3A, Table 1) are similar to those previously reported from this species (Clark and Dudley, 2010). When tested at backward airspeeds of 0–4.5 m s⁻¹, the power curve of a backward flying hummingbird resembled a hyperbola (Fig. 3B, Table 2), similar to the shape of the forward flight power curve at this range of airspeeds (Clark and Dudley, 2010).

Backward flight was characterized by significant increases in χ (Fig. 2A,C), λ_b and β_b compared with both hovering and forward flight (Table 1, Fig. 4A). Also, f increased significantly during backward flight, though only by 10% and 6% compared with forward and hovering flight, respectively (Table 1, Fig. 4B). β_h was reduced in backward flight compared with both hovering and forward flight, to such an extent that it became horizontal (Table 1, Fig. 4A). Φ declined slightly in backward flight compared with hovering, and $\Phi_{\max}:\Phi_{\min}$ significantly increased. J decreased significantly in backward flight relative to forward flight, whereas US:DS increased significantly in backward flight compared with either hovering or forward flight (Table 1, Fig. 4B).

For the bird tested while flying at variable backward airspeeds, χ consistently increased with airspeed, and also λ_b increased substantially at 4.5 m s⁻¹ relative to other airspeeds. β_b slightly increased with airspeed while β_h decreased, and reached a mean angle of -15 deg at a backward airspeed of 4.5 m s⁻¹ (Table 2, Fig. 5A). f substantially increased with airspeed, while Φ was almost constant at different airspeeds (Table 2, Fig. 5A). The same was true for both US:DS and $\Phi_{\max}:\Phi_{\min}$ with the exception of an increase in their values at 3 m s⁻¹ (Table 2, Fig. 5B). J decreased slightly, though consistently, with backward airspeed (Table 2).

Parasite power to overcome drag forces on the hummingbird model placed in forward and backward flight postures at an airspeed of 3 m s⁻¹ differed by only 0.6 mW between the two orientations. Despite the markedly different body postures during backward relative to forward flight, drag forces on the body were comparable at this relatively low airspeed (i.e. 12.9% and 16.5% of body weight for forward and backward flight, respectively).

DISCUSSION

Backward flight in hummingbirds is characterized by distinctive kinematic adjustments, some of which are not simple extrapolations from trends characterizing hovering and forward flight. A flattening of the stroke plane with respect to horizontal together with increased inclination of the stroke plane relative to the longitudinal body axis results in a dramatically steeper body posture. In conjunction with increased head flexion relative to the body, these features enable feeding while directing aerodynamic forces backward as well as upward. Because of the convergent evolution of hummingbirds and pterygote hexapods, we expect that similar kinematic adjustments will also be found in backward-flying insects that employ this unusual locomotor mode during station keeping, load lifting and predator evasion (see Frina et al., 1995; Nachtigall, 1998; Yokoi and Fujisaki, 2009; Zeil and Wittmann, 1989). Anecdotal observations of short backward flights in sunbirds (Nectariniidae, Passeriformes) (see Ng'weno, 1990) suggest that this locomotor mode may have more generally evolved in nectarivorous birds that frequently retreat in mid-air from flowers. Yet, while backward flight is usually a transient behavior in hummingbirds and other flying animals, the present study demonstrates that hummingbirds can successfully, and seemingly effortlessly, sustain backward flight during feeding.

Various kinematic changes associated with backward flight have been revealed in the present study. The relatively high χ and β_b in backward flight parallel the forward flight relationships for these variables found in rufous hummingbird (*Selasphorus rufus*), in which the two variables increased with decreasing forward airspeed from 12 to 0 m s⁻¹ (Tobalske et al., 2007). An upright body posture was described by earlier, and more qualitative, studies for backward flying hummingbirds (Greenewalt, 1960a), and also wasps (Nachtigall, 1998). This body posture likely involves higher drag (Greenewalt, 1960a) (but see below), yet it is the only means by which hummingbirds may be able to direct net aerodynamic forces upward and backward to overcome the simultaneous forces of gravity and body drag. Body angle relative to horizontal increased with increasing backward flight speed, while ventral head flexion increased concomitantly, thus enabling the bird's bill to be positioned horizontally (or nearly so) during feeding (Figs 4, 5, Tables 1, 2). β_h consistently decreased when forward flight speed decreased to the point of still-air hovering, and the same trend continued with an increase in backward flight speed. A similar trend with forward flight speed has been reported for rufous hummingbirds (Tobalske et al., 2007). This change is likely tightly linked to the direction of mean aerodynamic forces exerted during flight at different airspeeds,

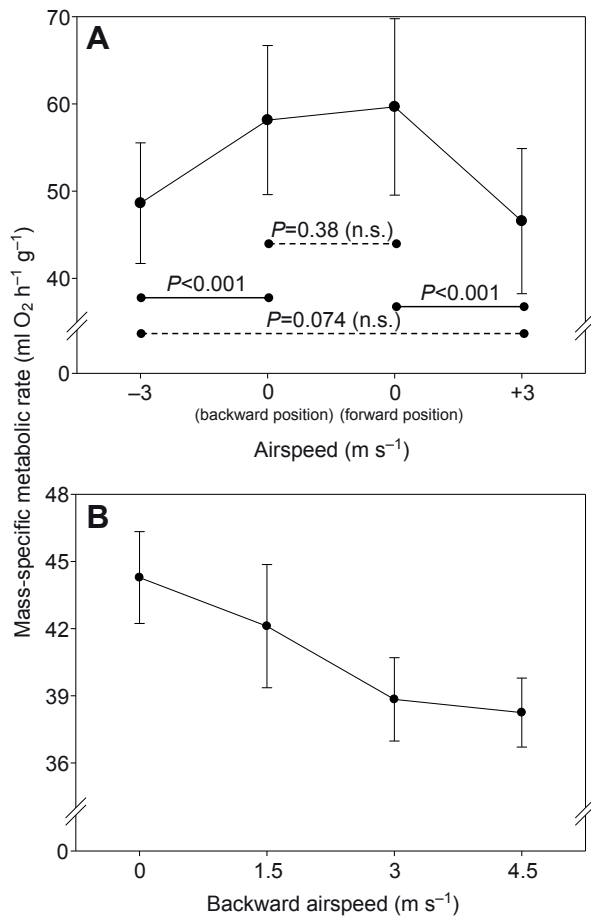


Fig. 3. Mass-specific metabolic rate (means \pm s.d.) for Anna's hummingbirds at different flight conditions. (A) Metabolic rate ($N=5$ individuals) during backward and forward flight at 3 m s^{-1} , and still-air hovering with the same feeder positions, including the results of Bonferroni *post hoc* comparisons following two-way mixed ANOVA. (B) Metabolic rate of an Anna's hummingbird during still-air hovering and backward flight at 1.5, 3.0 and 4.5 m s^{-1} airspeed.

as the bird needs to direct forces both forward and upward during forward flight.

Another intriguing aspect of the wingbeat kinematics associated with backward flight relates to observed variation in f . The $\sim 15\%$ increase in f with the decrease in forward flight speed and the increase in backward flight speed is relatively high for hummingbirds, otherwise known to have a rather invariant f (Clark and Dudley, 2010; Tobalske et al., 2007) to such an extent that it has been suggested not to differ by more than 5% during different flight behaviors (Greenewalt, 1960a; Greenewalt, 1960b). Regarding the duration of upstroke and downstroke throughout the wingbeat cycle, Tobalske and colleagues (Tobalske et al., 2007) suggested that this variable increases when forward airspeed decreases, and thus the high US:DS value found in backward flight may represent a continuation of this relationship into the effectively negative regions of the airspeed axis. Yet, inference regarding this variable should be made with caution, as the trend for this variable is not clear for the one bird that was measured over a full range of backward flight speeds. In this individual, US:DS was overall fairly low for 0 and 1.5 m s^{-1} backward flight, increased at a backward

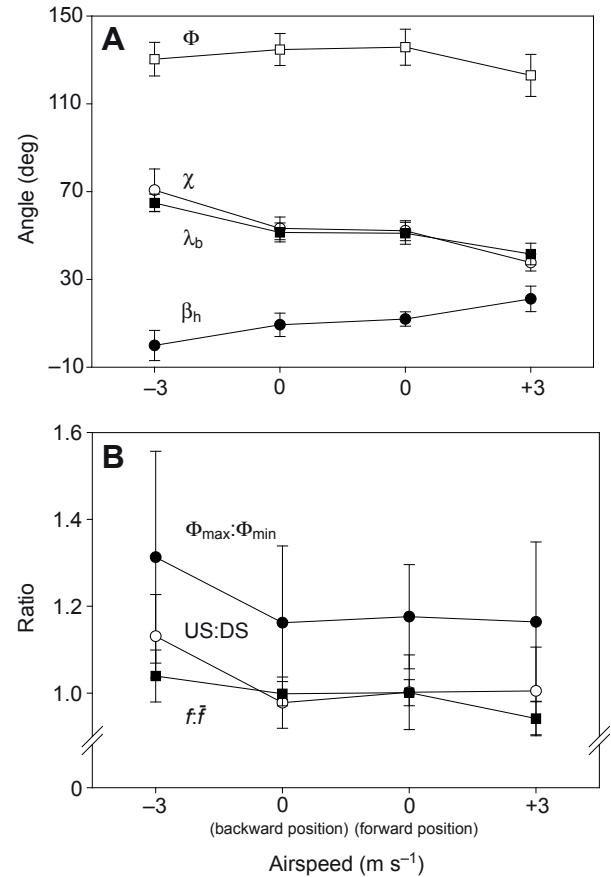


Fig. 4. Body and wingbeat kinematics (mean \pm s.d.) for Anna's hummingbirds ($N=5$ individuals) during backward and forward flight at 3 m s^{-1} , and still-air hovering with the same feeder positions. (A) Stroke plane angle in relation to horizontal (Φ ; filled circles), ventral head flexion in relation to longitudinal body axis (λ_b ; filled squares), body angle (χ ; open circles) and wingbeat amplitude (Φ ; open squares). (B) Ratio of wingbeat frequency to mean wingbeat frequency during hovering flight in still air ($f:\bar{f}$; filled squares), upstroke:downstroke duration ratio (US:DS; open circles) and ratio of maximum to minimum wing positional angle ($\Phi_{\max}:\Phi_{\min}$; filled circles).

speed of 3 m s^{-1} , and sharply decreased at 4.5 m s^{-1} . Possibly, more sampling may help decipher trends for this variable in relation to backward airspeed. Values of $\Phi_{\max}:\Phi_{\min}$ were high throughout the entire range of backward flight speeds, compared with hovering and forward flight, and may indicate a role for the mean positional angle of the wings in regulating torque and overall body angle. By contrast, values of Φ were high and almost constant regardless of flight directionality and airspeed in the Anna's hummingbird, whereas for rufous hummingbirds they were found to substantially increase with forward airspeed (Tobalske et al., 2007).

For the interpretation of backward flight in hummingbirds, one should also consider unique structural and skeletal features of hummingbirds and their neuromuscular control, primarily studied in still-air hovering (Hedrick et al., 2012; Warrick et al., 2012). The primary flight feathers of hummingbirds account for more than 75% of the wing area, a far higher proportion than in any other bird taxa (Greenewalt, 1960a; Warrick et al., 2012). This large handwing is highly rigid for different flight speeds throughout the flapping cycle (Tobalske et al., 2007), making hummingbird flight very different from other avian flight styles, more closely resembling insect-like

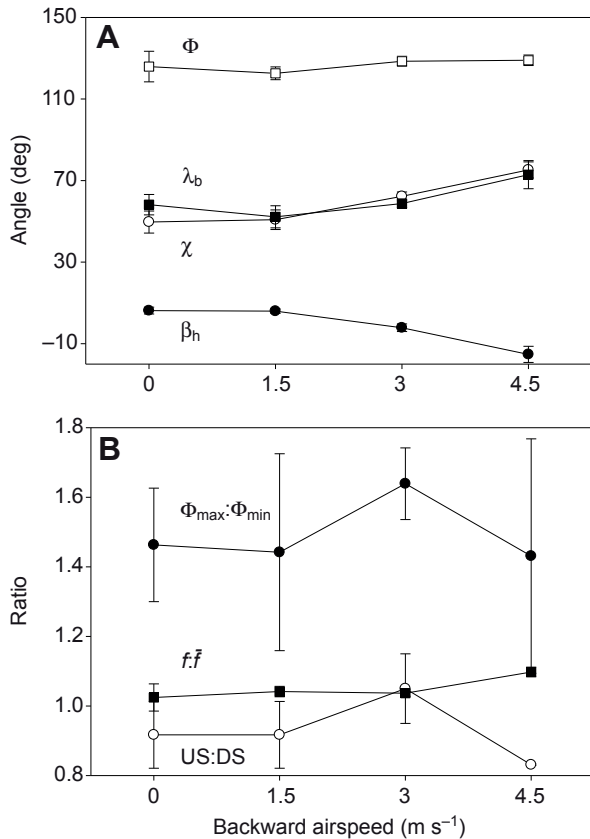


Fig. 5. Body and wingbeat kinematics (mean \pm s.d.) of an Anna's hummingbird during still-air hovering and backward flight at 1.5, 3.0 and 4.5 m s⁻¹ airspeed. (A) Stroke plane angle in relation to horizontal (β_h ; filled circles), ventral head flexion in relation to longitudinal body axis (λ_b ; filled squares), body angle (χ ; open circles) and wingbeat amplitude (Φ ; open squares). (B) Ratio of wingbeat frequency to mean wingbeat frequency during hovering flight in still air ($f:\bar{f}$; filled squares), upstroke:downstroke duration ratio (US:DS; open circles) and ratio of maximum to minimum wing positional angle ($\Phi_{\max}:\Phi_{\min}$; filled circles). The value of the mean wingbeat frequency (f_0) used here is taken from Fig. 4 and is not the f_0 calculated only from this particular bird.

flight (Dudley, 2000; Dudley, 2002; Altshuler and Dudley, 2002; Hedrick et al., 2012; Warrick et al., 2012). Based on evidence primarily from still-air hovering, Greenewalt (Greenewalt, 1960a; Greenewalt, 1960b) suggested that hummingbird flight may be best modeled by a mechanical oscillator. Some of the predictions of this mechanism, for example that the change in f at different flight behaviors and load-carrying conditions would be negligible compared with variation of other wingbeat kinematics such as Φ , have been generally supported in empirical studies (Chai and Dudley, 1995; Chai et al., 1997; Altshuler and Dudley, 2002; Altshuler and Dudley, 2003), and this was also found for hummingbirds flying at different forward flight speeds (Tobalske et al., 2007). Nevertheless, the present study shows very little variation in Φ at different flight conditions. In accordance with the findings of Tobalske and colleagues (Tobalske et al., 2007), variation in β_h is strikingly predictable throughout the range of studied flight speeds. In spite of differing kinematics, absolute values of the advance ratio J remained nearly constant during forward and backward flight over the studied speed range (Tables 1, 2), which likely derives from the limited range of airspeeds over which the

birds were flying [cf. Tobalske et al. (Tobalske et al., 2007), in which birds were flown at forward airspeeds of 0–12 m s⁻¹]. Wing movement in hummingbirds is achieved by a long-axis rotation of the humerus, with an important contribution from the shoulder's spherical rotation (Hedrick et al., 2012), albeit with a non-articulating wrist and elbow (Greenewalt, 1960a). Warrick and colleagues (Warrick et al., 2012) consequently suggested that such handwing inversion enables hummingbirds to effect a more completely reversed airfoil during the upstroke, presumably making their flight more efficient.

Here, alteration of the wing stroke plane such that it becomes horizontal or even directed upward in relation to horizontal during the downstroke is likely the key kinematic change that allows the bird to sustain feeding while flying backward. Both wingbeat amplitude and wing stroke plane in relation to the longitudinal body axis are relatively constant when flight mode changes from hovering to backward flight at increasingly higher speeds (Tables 1, 2). This likely results from features of shoulder joint rotation, or some other muscle–skeletal restriction (Hedrick et al., 2012). Under such conditions, the bird is probably forced to increase its projected body area and associated drag (but see below) by adopting a more upright body posture. Otherwise, it will not be able to maintain this 'reversed' wing stroke plane, and will consequently fail to sustain backward flight. However, hummingbirds also increased wingbeat frequency during backward flight (Table 2, Fig. 5), suggesting that the above-mentioned kinematic changes alone may not suffice to produce the lift and net vertical forces required for this type of flight.

The relatively low flight metabolic rate during backward flight, similar to that during forward flight, is surprising given the increase in projected body area relative to flow deriving from the more upright posture of the bird. However, this change in posture translates to only a slight increase in parasite power. Consequently, the overall reduction in power expenditure enjoyed during slow forward flight (Clark and Dudley, 2010) is similarly realized in backward flight, rendering it metabolically frugal compared with hovering. Flight metabolic rate decreases with airspeed in backward flight up to a speed of 4.5 m s⁻¹ (Fig. 3B), but it is unknown whether this trend holds true at higher backward airspeeds because backward flight could not be sustained at airspeeds >4.5 m s⁻¹. Consequently, we could not test whether the backward power input of Anna's hummingbird increases at high airspeeds, as documented in fast forward flight for this (Clark and Dudley, 2010) and many other bird species (e.g. Pennycuick, 1968; Rayner, 1999; Tobalske et al., 2003). Nevertheless, given the transient nature of this flight behavior under most circumstances for hummingbirds in the wild, and the relatively low backward flight speeds measured for a single hummingbird in the laboratory in still-air conditions (1.1–2.0 m s⁻¹, $N=3$, N.S., unpublished data), hummingbirds probably only rarely engage in backward flight at speeds close to their upper limit.

Another peculiarity of backward flight in Anna's hummingbirds relates to the relationship between f and \dot{V}_{O_2} . Using wind tunnel measurements, Pennycuick and colleagues (Pennycuick et al., 1996) showed that these two variables are related throughout a range of forward flight speeds, and that both have a U-shaped relationship with airspeed, with a minimum at the same airspeed. Consequently, one can be substituted for the other as a qualitative measure of the relationship between one of these variables and airspeed. For example, inference on the effects of drag resulting from a backpack transmitter on flight metabolism, and consequent migration range and lipid reserves at the end of migration, was based upon the above-mentioned relationship for rose-colored starlings (*Sturnus roseus*) whose wingbeat frequency was determined under different drag

treatments (Pennycuik et al., 2012). Hummingbirds are known to change their f only a little (Greenewalt, 1960a; Greenewalt, 1960b; Tobalske et al., 2007) while their \dot{V}_{O_2} substantially varies with airspeed (Clark and Dudley, 2010), and this may be attributed to the different way their flapping mechanism operates compared with other bird species (Greenewalt, 1960a; Greenewalt, 1960b; Dudley, 2000; Dudley, 2002; Tobalske et al., 2007; Hedrick et al., 2012; Warrick et al., 2012). The two variables were not related at all to each other in the present study, as \dot{V}_{O_2} was found to be similar for backward and forward flight at equivalent airspeeds, while f was higher during backward flight. Moreover, when tested throughout a range of backward flight speeds, f increased while \dot{V}_{O_2} decreased.

Hummingbirds in forward and backward flight at 3 m s^{-1} produced similar net forces, given that drag forces on the body were small relative to body weight. Calculating the aerodynamic force vector as the vector sum of the drag and the body weight, total force output increased by only about 1% at each body orientation relative to that in hovering flight. The induced power output is thus likely to be comparable in forward and backward flight at 3 m s^{-1} , and will necessarily decrease relative to hovering flight (see Rayner, 1988; Pennycuik, 2008). Moreover, the advance ratio J for the wings was also comparable in the two cases (see Table 1), suggesting that profile power will be of similar magnitude, and that trends in the power curve with airspeed will be driven primarily by the reduction in induced power given that parasite power was estimated to be negligible at the study airspeed. Consequently, the metabolic input during either forward or backward slow flight is expected to be lower than that during hovering, as was found in our study (see also Clark and Dudley, 2010). This observation necessarily assumes a constant flight muscle efficiency for all cases, but dramatic changes in this feature would be unlikely given the small magnitude of observed changes in wingbeat kinematics and, by inference, in muscle contraction parameters (see Table 1).

The use of wind tunnels is a common albeit not perfect practice to simulate natural free flight in volant taxa (see Engel et al., 2010). Since the pioneering study of Tucker (Tucker, 1966; Tucker, 1968), many researchers have quantified avian flight energetics within wind tunnels using different species and behavioral contexts (e.g. Baudinette and Schmidt-Nielsen, 1974; Bundle et al., 2007; Butler et al., 1977; Hudson and Bernstein, 1983; Torre-Bueno and Larochelle, 1978; Tucker, 1972; Ward et al., 2004). Unlike most other bird species, hummingbirds do not require training to fly within experimental volumes because of their attraction to nectar-bearing flowers or artificial mimics thereof. Welch suggested that mask respirometry is a highly reliable technique for extracting metabolic measurements from hummingbirds either in the laboratory or in the field, and that (unlike tethered respirometry) this method elicits sustained, steady and voluntary flights (Welch, 2011). Consequently, mask respirometry studies have shed light on diverse aspects of avian physiology and behavior, and have enabled important inferences on the mechanisms and consequences of bird flight (see Welch, 2011). Although it is possible that the flight-feeding behaviors studied here differ from either free hovering or forward and backward flight in the wild, we suggest that the low range of flight speeds studied here will yield very similar kinematics and mechanics. At higher speeds (e.g. $>5 \text{ m s}^{-1}$), the greater demands of maintaining stability at the feeder in the face of endogenous flow perturbations (i.e. turbulence) may impinge correspondingly on flight biomechanics and energetics.

Backward flight is a behavior that renders immediate turning after feeding from a flower unnecessary. As such, it can be viewed as one of the many adaptations [e.g. the physiological oxidation cascade of sugars (see Suarez et al., 2011) and the rigidity of the wing (see

Greenewalt, 1960a; Greenewalt, 1960b; Dudley, 2002; Warrick et al., 2012)] that are associated with hummingbird flight in general, and with their aerial feeding in particular. Also, aerial agility in hummingbirds yields rapid changes in body translation and rotation that are likely unmatched by any other avian taxon (see Altshuler and Dudley, 2002; Dudley, 2002). In the context of the present study, our understanding of hummingbird axial agility and their flight envelope more generally should now be extended to include controlled backward accelerations and sustained backward flight. It will be particularly interesting in future work to determine the contribution of this flight mode to various behavioral situations (e.g. agonistic interactions, predation) for which selection is particularly potent.

LIST OF SYMBOLS AND ABBREVIATIONS

f	wingbeat frequency
$F_{E_{O_2}}$	fractional concentration of O_2 exiting the mask
$F_{I_{O_2}}$	fractional concentration of O_2 entering the mask
J	advance ratio
R	wing length
US:DS	upstroke to downstroke duration ratio
\dot{V}_E	mass flow of gas exiting the respirometry mask
\dot{V}_{O_2}	rate of oxygen consumption
β_b	stroke plane angle in relation to longitudinal body axis
β_h	stroke plane angle in relation to horizontal
χ	body angle in relation to horizontal
λ_b	head flexion in relation to the longitudinal body axis
Φ	wingbeat amplitude
$\Phi_{\max}:\Phi_{\min}$	ratio of maximum to minimum wing positional angle

ACKNOWLEDGEMENTS

We are grateful for the assistance of Dennis Evangelista, Erica Kim and other members of the Animal Flight Laboratory at UC Berkeley.

FUNDING

This study was supported by the National Science Foundation, Division of Integrative Organismal Systems [grant number 0837866].

REFERENCES

- Altshuler, D. L. and Dudley, R. (2002). The ecological and evolutionary interface of hummingbird flight physiology. *J. Exp. Biol.* **205**, 2325-2336.
- Altshuler, D. L. and Dudley, R. (2003). Kinematics of hovering hummingbird flight along simulated and natural elevational gradients. *J. Exp. Biol.* **206**, 3139-3147.
- Ashley-Ross, M. A. and Lauder, G. V. (1997). Motor patterns and kinematics during backward walking in the pacific giant salamander: evidence for novel motor output. *J. Neurophysiol.* **78**, 3047-3060.
- Askew, G. N. and Ellerby, D. J. (2007). The mechanical power requirements of avian flight. *Biol. Lett.* **3**, 445-448.
- Bartholomew, G. A. and Lighton, J. R. B. (1986). Oxygen consumption during hovering in free-ranging Anna hummingbirds. *J. Exp. Biol.* **123**, 191-199.
- Baudinette, R. V. and Schmidt-Nielsen, K. (1974). Energy cost of gliding flight in herring gulls. *Nature* **248**, 83-84.
- Berger, M. and Hart, J. S. (1972). Respiration in hummingbird *Amazilia fimbriata* during hovering at different ambient temperatures. *J. Comp. Physiol. A* **81**, 363-380.
- Buford, J. A. and Smith, J. L. (1990). Adaptive control for backward quadrupedal walking. II. Hindlimb muscle synergies. *J. Neurophysiol.* **64**, 756-766.
- Bundle, M. W., Hansen, K. S. and Dial, K. P. (2007). Does the metabolic rate-flight speed relationship vary among geometrically similar birds of different mass? *J. Exp. Biol.* **210**, 1075-1083.
- Butler, P. J., West, N. H. and Jones, D. R. (1977). Respiratory and cardiovascular responses of the pigeon to sustained, level flight in a wind-tunnel. *J. Exp. Biol.* **71**, 7-26.
- Cavagna, G. A., Legramandi, M. A. and La Torre, A. (2011). Running backwards: soft landing-hard takeoff, a less efficient rebound. *Proc. R. Soc. Lond. B* **278**, 339-346.
- Cavagna, G. A., Legramandi, M. A. and La Torre, A. (2012). An analysis of the rebound of the body in backward human running. *J. Exp. Biol.* **215**, 75-84.
- Chai, P. and Dudley, R. (1995). Limits to vertebrate locomotor energetics suggested by hummingbirds hovering in heliox. *Nature* **377**, 722-725.
- Chai, P., Chen, J. S. C. and Dudley, R. (1997). Transient hovering performance of hummingbirds under conditions of maximal loading. *J. Exp. Biol.* **200**, 921-929.
- Clark, C. J. and Dudley, R. (2010). Hovering and forward flight energetics in Anna's and Allen's hummingbirds. *Physiol. Biochem. Zool.* **83**, 654-662.
- Davey, W. N. and Davey, J. R. (1945). Hovering and backward flight in the hummingbird. *Jack Pine Warbler* **23**, 2-7.

- Dial, K. P., Biewener, A. A., Tobalske, B. W. and Warrick, D. R. (1997). Mechanical power output of bird flight. *Nature* **390**, 67-70.
- Dudley, R. (1992). Aerodynamics of flight. In *Biomechanics: A Practical Approach* (ed. A. A. Biewener), pp. 97-121. New York: Oxford University Press.
- Dudley, R. (2000). *The Biomechanics of Insect Flight: Form, Function, Evolution*. Princeton, NJ: Princeton University Press.
- Dudley, R. (2002). Mechanisms and implications of animal flight maneuverability. *Integr. Comp. Biol.* **42**, 135-140.
- Ellington, C. P. (1984). The aerodynamics of hovering insect flight. III. kinematics. *Philos. Trans. R. Soc. Lond. B* **305**, 41-78.
- Engel, S., Bowlin, M. S. and Hedenström, A. (2010). The role of wind-tunnel studies in integrative research on migration biology. *Integr. Comp. Biol.* **50**, 323-335.
- Flynn, T. W., Connery, S. M., Smutok, M. A., Zeballos, R. J. and Weisman, I. M. (1994). Comparison of cardiopulmonary responses to forward and backward walking and running. *Med. Sci. Sports Exerc.* **26**, 89-94.
- Frina, W. M., Kramer, D. and Varjú, D. (1995). The response of the hovering hawk moth *Macroglossum stellatarum* to translatory pattern motion. *J. Comp. Physiol. A* **176**, 551-562.
- Grasso, R., Bianchi, L. and Lacquaniti, F. (1998). Motor patterns for human gait: backward versus forward locomotion. *J. Neurophysiol.* **80**, 1868-1885.
- Greenewalt, C. H. (1960a). *Hummingbirds*. New York: Doubleday.
- Greenewalt, C. H. (1960b). The wings of insects and birds as mechanical oscillators. *Proc. Am. Philos. Soc.* **104**, 605-611.
- Hedrick, T. L., Tobalske, B. W., Ros, I. G., Warrick, D. R. and Biewener, A. A. (2012). Morphological and kinematic basis of the hummingbird flight stroke: scaling of flight muscle transmission ratio. *Proc. R. Soc. Lond. B* **279**, 1986-1992.
- Hudson, D. M. and Bernstein, M. H. (1983). Gas exchange and energy cost of flight in the white-necked raven, *Corvus cryptoleucus*. *J. Exp. Biol.* **103**, 121-130.
- Lighton, J. R. B. (2008). *Measuring Metabolic Rates: a Manual for Scientists*. New York: Oxford University Press.
- Nachtigall, W. (1998). Landing- and take-off flight behaviour of the potter wasp *Odynerus reniformis* at its nesting tube with and without a load (Hymenoptera: Eumenidae). *Entomol. Gen.* **22**, 177-198.
- Ngweno, F. (1990). Sunbird flying backwards? *East Africa Nat. Hist. Bull.* **20**, 27-28.
- Pennycuik, C. J. (1968). Power requirements for horizontal flight in the pigeon *Columba livia*. *J. Exp. Biol.* **49**, 527-555.
- Pennycuik, C. J. (2008). *Modelling the Flying Bird*. New York: Academic Press.
- Pennycuik, C. J., Klaassen, M., Kvist, A. and Lindström, Å. (1996). Wingbeat frequency and the body drag anomaly: wind-tunnel observations on a thrush nightingale (*Luscinia luscinia*) and a teal (*Anas crecca*). *J. Exp. Biol.* **199**, 2757-2765.
- Pennycuik, C. J., Fast, P. L. F., Ballerstädt, N. and Rattenborg, N. (2012). The effect of an external transmitter on the drag coefficient of a bird's body, and hence on migration range, and energy reserves after migration. *J. Ornithol.* **153**, 633-644.
- Rayner, J. M. V. (1988). Form and function in avian flight. *Curr. Ornithol.* **5**, 1-77.
- Rayner, J. M. V. (1999). Estimating power curves of flying vertebrates. *J. Exp. Biol.* **202**, 3449-3461.
- Siegel, S. and Castellan, N. J., Jr (1988). *Nonparametric Statistics for the Behavioral Sciences*. New York: McGraw-Hill.
- Suarez, R. K., Herrera M, L. G. and Welch, K. C., Jr (2011). The sugar oxidation cascade: aerial refueling in hummingbirds and nectar bats. *J. Exp. Biol.* **214**, 172-178.
- Tobalske, B. W., Hedrick, T. L., Dial, K. P. and Biewener, A. A. (2003). Comparative power curves in bird flight. *Nature* **421**, 363-366.
- Tobalske, B. W., Warrick, D. R., Clark, C. J., Powers, D. R., Hedrick, T. L., Hyder, G. A. and Biewener, A. A. (2007). Three-dimensional kinematics of hummingbird flight. *J. Exp. Biol.* **210**, 2368-2382.
- Torre-Bueno, J. R. and Larochele, J. (1978). The metabolic cost of flight in unrestrained birds. *J. Exp. Biol.* **75**, 223-229.
- Tucker, V. A. (1966). Oxygen consumption of a flying bird. *Science* **154**, 150-151.
- Tucker, V. A. (1968). Respiratory exchange and evaporative water loss in flying budgerigar. *J. Exp. Biol.* **48**, 67-87.
- Tucker, V. A. (1972). Metabolism during flight in the laughing gull, *Larus atricilla*. *Am. J. Physiol.* **222**, 237-245.
- Vilensky, J. A. and Cook, J. A. (2000). Do quadrupeds require a change in trunk posture to walk backward? *J. Biomech.* **33**, 911-916.
- Vilensky, J. A., Gankiewicz, E. and Gehlsen, G. (1987). A kinematic comparison of backward and forward walking in humans. *J. Hum. Mov. Stud.* **13**, 29-50.
- Walsberg, G. E. and Wolf, B. O. (1995). Variation in the respiratory quotient of birds and implications for indirect calorimetry using measurements of carbon dioxide production. *J. Exp. Biol.* **198**, 213-219.
- Ward, S., Möller, U., Rayner, J. M. V., Jackson, D. M., Nachtigall, W. and Speakman, J. R. (2004). Metabolic power of European starlings *Sturnus vulgaris* during flight in a wind tunnel, estimated from heat transfer modelling, doubly labelled water and mask respirometry. *J. Exp. Biol.* **207**, 4291-4298.
- Warrick, D., Hedrick, T., Fernández, M. J., Tobalske, B. and Biewener, A. (2012). Hummingbird flight. *Curr. Biol.* **22**, R472-R477.
- Welch, K. C., Jr (2011). The power of feeder-mask respirometry as a method for examining hummingbird energetics. *Comp. Biochem. Physiol.* **158A**, 276-286.
- Welch, K. C., Jr, Altshuler, D. L. and Suarez, R. K. (2007). Oxygen consumption rates in hovering hummingbirds reflect substrate-dependent differences in P/O ratios: carbohydrate as a 'premium fuel'. *J. Exp. Biol.* **210**, 2146-2153.
- Williford, H. N., Olson, M. S., Gauger, S., Duey, W. J. and Blessing, D. L. (1998). Cardiovascular and metabolic costs of forward, backward, and lateral motion. *Med. Sci. Sports Exerc.* **30**, 1419-1423.
- Winter, D. A., Pluck, N. and Yang, J. F. (1989). Backward walking: a simple reversal of forward walking? *J. Mot. Behav.* **21**, 291-305.
- Withers, P. C. (1977). Measurement of V_{O_2} , V_{CO_2} , and evaporative water loss with a flow-through mask. *J. Appl. Physiol.* **42**, 120-123.
- Yokoi, T. and Fujisaki, K. (2009). Hesitation behaviour of hoverflies *Sphaerophoria* spp. to avoid ambush by crab spiders. *Naturwissenschaften* **96**, 195-200.
- Zeil, J. and Wittmann, D. (1989). Visually controlled station-keeping by hovering guard bees of *Trigona (Trigona) angustula* (Apidae, Meliponinae). *J. Comp. Physiol. A* **165**, 711-718.